Magnetically Recoverable Catalysts for Cellulose and Inulin Conversion

Esther Sulman[a], Oleg Manaenkov[a,*], Olga Kislitsa[a], Ekaterina Ratkevich[a], Mikhail Sulman[a], Valentina Matveeva[b]

[a]Tver State Technical University, Russian Federation
[b]Tver State University, Russian Federation
 ovman@yandex.ru

A new Ru-containing catalyst based on Fe_3O_4-SiO_2 particles that exhibit magnetic properties is proposed for the hydrogenolysis of cellulose to glycols and the hydrolytic hydrogenation of inulin to mannitol. Here, we also report utilisation of a magnetically recoverable catalyst in the inulin hydrolytic hydrogenation to mannitol. The effect of process parameters on the selectivity toward the main products is studied. In the hydrogenolysis of cellulose, the highest selectivities for EG (19.1 %) and PG (20.9 %) are achieved within 50 min under conditions of 255 °C, H_2 60 bar. The conversion of cellulose is 100 %. In the hydrolytic hydrogenation of inulin, maximum mannitol selectivity (44.3 %) is reached within 45 min under conditions of 150 °C, H_2 60 bar. The conversion of inulin is 100 %.The catalyst used in this work is stable under hydrothermal conditions of the process. It can be easily magnetically separated from the reaction mixture and reused without any loss of selectivity and activity, making this catalyst promising for practical applications in biomass conversion.

1. Introduction

Polyols are an important platform chemicals; they are commonly used in different branches of modern industry. Ethylene glycol (EG) and propylene glycol (PG) are used in manufacturing medicines, fuels, surfactants, antifreezes, lubricants (Yue et al., 2012), and solvents (Harlin A., 2011). Propylene glycol is also used for the synthesis of lactic acid, which is used in the production of biodegradable polylactones (Sugiyama et al., 2013). EG and PG can be obtained via cellulose hydrogenolysis in subcritical water in the presence of heterogeneous catalysts (Manaenkov et al., 2019). Mannitol, $C_6H_{14}O_6$, is employed in pharmaceutical (Okoromah et al., 2011), chemical (Prabhakar et al., 2014), and food industry as well as in biotechnology (Bereczki et al., 2007). It is used to treat brain diseases as a food supplement (E421) and a sweetener in diabetic foods (Lawson et al., 2007), in the production of resins, linseed oil, coatings, surfactants, explosives (Imhof et al., 2013), and cosmetics (Ohrem et al., 2014). Nontoxic and inexpensive mannitol can be utilised as a phase change material for latent heat storage (Alva et al., 2018). These applications determine the high demand for mannitol. There are numerous methods for mannitol syntheses. It can be obtained by electrolytic reduction of glucose or by hydrogenation of invert sugars, monosaccharides, or sucrose (Budavari, 1996). The shortcoming of the above methods is that they use food sugars, and interfering with the food supply. This makes the development of novel, effective methods for mannitol syntheses using non-food polysaccharides a high priority (Rinaldi, 2014). One of such methods is the hydrolytic hydrogenation of inulin (Heinen et al., 2001). Inulin is a naturally occurring polysaccharide, widely available as plant biomass (Pinheiro et al., 2011) and used in food biotechnology (Mayuri et al., 2017).

The inulin hydrolytic hydrogenation can be carried out as a one-pot procedure in the presence of heterogeneous catalysts containing various precious metals. The reaction is carried out in subcritical water, which is both a hydrolysis catalyst and a reagent. Because polysaccharide (including inulin) hydrolysis in subcritical water is fast, the hydrolytic hydrogenation efficiency is mainly determined by the activity of the hydrogenation catalyst. Ru-containing catalysts are considered most active in hydrolytic hydrogenation and hydrogenolysis (Matveeva et al., 2017).

Magnetically separable catalysts received considerable attention due to easy magnetic separation from reaction mixtures, facilitating the catalyst repeated use and allowing one to save energy and materials, decreasing the target product costs (Wang et al., 2014a). To date, Ru-containing magnetically separable catalysts have been used in olefin metathesis, azide-alkyne cycloaddition, hydrogenation, oxidation, etc. (Wang et al., 2014b). Among other reactions where such catalysts were employed, the biomass conversion is one of the most promising for utilising renewable resources. Magnetically separable catalysts have shown good results in cellulose conversion (Zhang et al., 2014).

In this work, a Ru-containing catalyst based on Fe_3O_4-SiO_2 particles exhibiting magnetic properties is proposed for the hydrogenolysis of cellulose to glycolsand the hydrolytic hydrogenation of inulin.

2. Experimental

2.1 Materials

Iron (III) nitrate, mesoporous silica gel (6 nm porosity, 200-425 mesh particle size) and ruthenium (III) acetylacetonate ($Ru(acac)_3$, 97 %) were purchased from Sigma-Aldrich and used without purification. Ethylene glycol (99.0 %) and tetrahydrofuran (THF) were purchased from Macron Fine Chemicals and used as received. Inulin (99 %) was purchased from TCI (Japan) and used without purification.

2.2 The catalyst synthesis

In a typical synthesis, to the solution of 2 g of $Fe(NO_3)_3$ dissolved in 10 mL of ethanol, 2.5 g of silica gel was added. The mixture was allowed to stir overnight in air for ethanol evaporation. The sample was then dried in a vacuum oven at room temperature for a minimum of 2 hours. The powder was then stirred with a spatula, adding 25 drops of ethylene glycol. This sample was then loaded into two porcelain boats and heated in a quartz tube under argon to 250 °C with a heating rate of 2 °C/min. The heating at 250 °C was held for 5 h and then the sample was cooled to room temperature.

$Ru(acac)_3$ (0.495 g) was dissolved in 10 mL of THF and mixed with Fe_3O_4-SiO_2 prepared in the previous step. The suspension was stirred overnight in air to allow THF evaporation. The sample was then dried in vacuum at room temperature until it was entirely dry. The powdered product was stirred with 25 drops of ethylene glycol. The sample was then loaded into two porcelain boats and heated in a quartz tube in a tube furnace under argon to 300 °C with a heating rate of 2 °C/min followed by 3 h heating at this temperature. After that the product was allowed to cool to room temperature.

Reduction of this sample was carried out before catalytic experiments by hydrogen at 300 °C for 2 h. After cooling the catalyst was stored in a sealed container at room temperature.

2.3 Characterization

The transmission electron microscopy (TEM) images were acquired on a JEOL JEM1010 transmission electron microscope. Images were analysed with image-processing package ImageJ to estimate nanoparticle diameters. High resolution TEM (HRTEM) images and scanning TEM (STEM) energy dispersive X-ray spectra (EDS) were acquired at an accelerating voltage of 300 kV on a JEOL 3200FS transmission electron microscope equipped with an Oxford Instruments INCA EDS system. The same TEM grids were used for all analyses. X-ray fluorescence (XRF) measurements to determine the Ru content were performed with a Zeiss Jena VRA-30 spectrometer. Atomic adsorption spectrometry (AAS) to determine Ru and Fe contents in the liquid phase after a catalytic reaction was carried out MGA-915 (Lumex, Russia), equipped with hollow cathode lamps for Ru (349.9 nm) and Fe (248.3 nm).

2.4 Experimental procedure

Our tests were conducted in a 50 cm^3 high-pressure steel reactor (Parr Instruments, United States) equipped with a PARR 4843 controller and a propeller stirrer. In a typical test, the polysaccharide, the catalyst, and 30 mL of distilled water were placed into the reactor. The reactor was triply purged with hydrogen at a pressure of 60 bar; heating and stirring (≈ 100 rpm) were then switched on to prevent the formation of local zones of overheating and the saturation of the catalyst surface with hydrogen. Upon reaching the operational temperature, the speed of the stirrer was increased to 600 rpm. This time was considered to be the starting point of the test. After each test, the catalyst was separated from the reaction mass using a neodymium magnet.

The liquid phase of the catalyst was analysed on an UltiMate 3,000 liquid chromatograph (Dionex, United States) equipped with a refractometric detector. Polysaccharide conversion was calculated using the formula $X = [(m_{p0} - m_p)/m_{p0}] \times 100$ %, where m_p is the weight of the polysaccharide residue after the reaction and m_{p0} is the initial weight of the polysaccharide. Selectivity was calculated with the formula $S = [m_{pr}/(m_{p0} - m_p)] \times 100$ %, where m_{pr} is the weight of the respective product.

3. Results and discussion

3.1 Catalyst characterization

Figure 1 displays the TEM image of 5 % $Ru-Fe_3O_4-SiO_2$ and its EDS spectrum. The EDS spectrum shows Ru, Fe, Si, and O from the catalyst, Cu from the TEM grid and Cr from the grid holder. TEM and HRTEM images confirm the presence of nanoparticles. While the iron oxide NP diameter is difficult to determine from TEM because of the low electron contrast difference between iron oxide and silica, the Ru-containing nanoparticles were measured and showed a diameter of 2.0 nm. The XRD pattern of this sample displays a broad signal at approximately 22 degrees two theta which is due to amorphous silica and the set of reflections that is typical of that of magnetite (Guivar et al., 2014). Analogous XRD pattern is observed for $Fe_3O_4-SiO_2$ (Figure 1c). The magnetite crystallite size calculated using Scherrer's formula for the (311) reflection is 12.3 nm. Considering that the magnetite NPs are located in the 6 nm silica pores (Figure 1a), it is surprising that the crystallite size is larger by a factor of 2. We assume that two or more magnetite NPs are connected due to oriented attachment, forming larger single crystals.
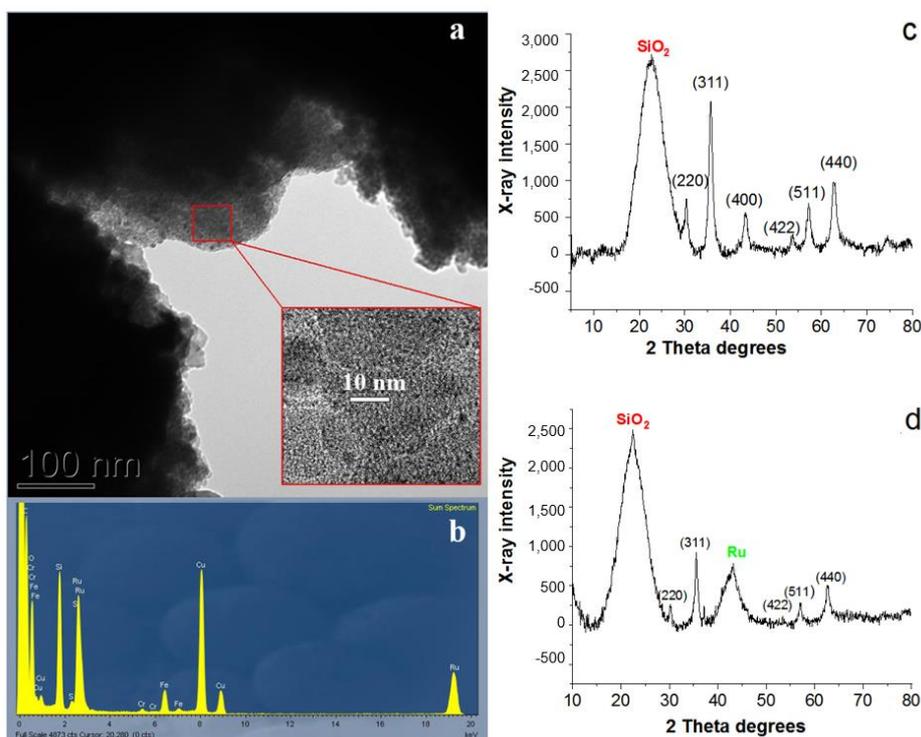
Figure 1: TEM image (a), EDS spectrum (b), and XRD pattern (d) of 5 % Ru- $Fe_3O_4-SiO_2$. XRD pattern of Fe_3O_4-SiO_2 is shown in (c) for comparison. Inset in (a) shows the HRTEM image

It is worth noting that the (400) reflection of magnetite is overlapped with the (101) reflection of the Ru (0) phase. The X-ray photoelectron spectroscopy (XPS) data presented in our preceding paper (Manaenkov et al., 2016) demonstrated the presence of Ru (IV) and Ru (0) species at the 1/1 atomic ratio, indicating that the RuO^2 phase is amorphous. It is worth noting that the XPS is a surface method, allowing one to conclude that RuO_2 is most likely located on the nanoparticle surface. Liquid nitrogen adsorption measurements show that for $Fe_3O_4-SiO_2$ and 5 % Ru- $Fe_3O_4-SiO_2$, the BET surface areas are 304 m^2/g and 280 m^2/g, indicating that the incorporation of Ru-containing NPs in the magnetic silica pores decreases the surface area by ~8 %.

3.2 Cellulose hydrogenolysis

A catalyst of 5 % $Ru-Fe_3O_4-SiO_2$ was used in the hydrogenolysis of microcrystalline cellulose to glycols. A previously developed catalyst based on hypercrosslinked polystyrene (HPS) – 3 % Ru/HPS MN270 – was used for comparison (Matveeva et al., 2017). The main products of cellulose hydrogenolysis are EG (selectivity of 10–19 %, depending on the reaction conditions) and PG (15–23 %). Small amounts of glycerol (up to 5 %), sorbitol (up to 4 %), mannitol (up to 2 %), and xylitol (up to 1 %) also form. Chromatography–mass spectrometry analysis showed that the liquid phase contained trace amounts of 1,4-sorbitan, hexane-1,2,5,6-tetraol, hexane-

1,2,3,4,5-pentanol, and some other products. Our study revealed that the optimum ratio between Ru (in the catalyst's composition) and cellulose is 0.1167 : 1 (mmol/g). This optimum is due to the following reasons. At low Ru contents, the yield of C_6–C_3 polyols grows with a simultaneous drop in the yield of EG and PG. An increase in the Ru content also reduces the yield of EG and PG; this finding can be attributed to the subsequent hydrogenolysis of these products to ethanol, methanol, and methane. The temperature dependence of cellulose conversion is shown in Figure 2a. At 240°C, the conversion reaches 100 % within 60 min. The effect of the temperature on glycol selectivity is shown in Figure 2b. The highest selectivity toward EG and PG is observed at 255 °C (12 and 22 %). In a temperature range of 205–235 °C, the selectivities toward EG and PG remain low, while C_6–C_3 polyols are present in the catalysate in considerable amounts, testifying to the low degree of these materials' hydrogenolysis. At 235 °C in particular, sorbitol selectivity was 4.3 %, while the selectivities toward mannitol, 1,4-sorbitan, xylitol, and erythritol lie in the range of 1.1–1.3 %. At temperatures above 255 °C, EG selectivity diminishes, while PG selectivity remains virtually the same.

(a)   (b)
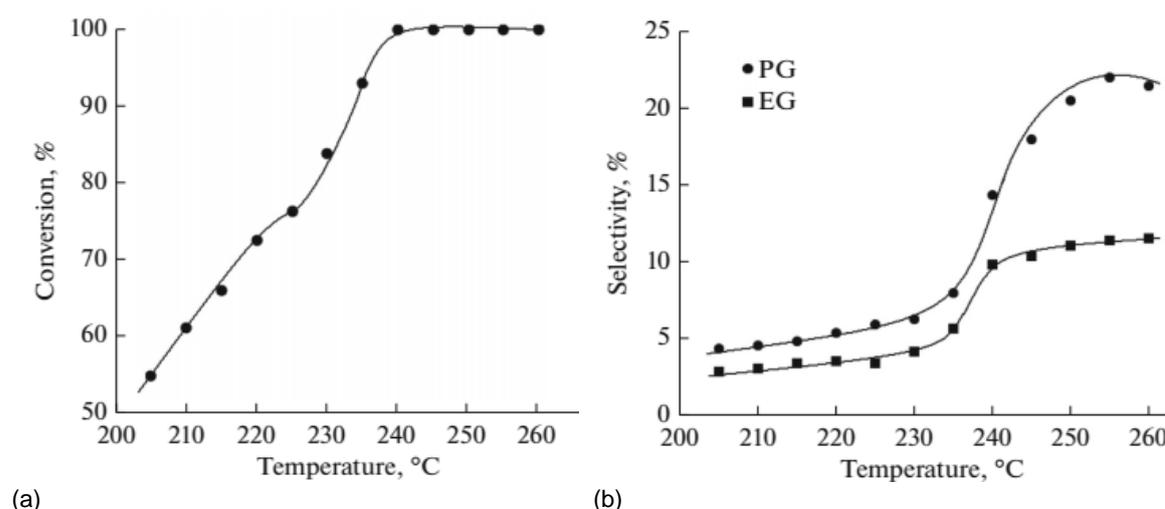
Figure 2: (a) Cellulose conversion as functions of the process temperature (0.1167 mmol of Ru per gram of cellulose; 0.3 g of cellulose; 0.07 g of catalyst; 30 mL of H_2O; = 60 bar, 60 min) (b) EG and PG selectivity as functions of the process temperature (0.1167 mmol of Ru per gram of cellulose; 0.3 g of cellulose; 0.07 g of catalyst; 30 mL of H_2O; = 60 bar, 60 min)

The dependence of cellulose conversion and the selectivity toward the main products on the process time was studied. The highest glycol selectivity was observed at a reaction time of 30 min, but the amount of C_6–C_3 polyols was still considerable. By the 50th minute, these alcohols were barely present in the reaction mixture. 100 % cellulose conversion was observed even after 20 min of the test.

Table 1: Productivity (A_k) and glycol selectivity (S) for 5 % Ru-Fe_3O_4-SiO_2 and the reference catalyst[a]

Catalyst	A_k (product weight/catalyst weight per hour), h^{-1}		S, %	
	EG	PG	EG	PG
5 % Ru-Fe_3O_4-SiO_2	0.62	1.18	12.0	22.9
5 % Ru-Fe_3O_4-SiO_2[b]	0.99	1.08	19.1	21.0
3 % Ru/HPS MN270	0.22	0.38	7.2	12.3

[a]0.1167 mmol of Ru per gram of cellulose; 0.3 g of cellulose; 30 mL of H_2O; 255 °C; 60 bar H_2; 50 min
[b]0.195 mol of Ca(OH)$_2$ per mol of cellulose

Table 1 lists the productivities (activity Ak) of the catalysts and the glycol selectivity under optimum reaction conditions. The data in Table 1 show the productivity of the magnetically recoverable catalyst was approximately three times higher than that of the 3 % Ru/HPS MN270 catalyst, which earlier showed good results in thehydrolytic hydrogenation of cellulose to sorbitol (Matveeva et al., 2017). It was shown that adding a retroaldol cleavage catalyst (Ca(OH)$_2$) to the reaction mixture increased the yield of EG.

To study its stability, the 5 % Ru-Fe_3O_4-SiO_2 catalyst was separated from the reaction medium using a neodymium magnet and used in the next test with a fresh portion of cellulose, distilled water, and Ca(OH)$_2$. The

selectivity toward EG and PG and the productivity of the catalyst remained virtually the same, testifying to the stability of the catalyst under the hydrothermal conditions of cellulose hydrogenolysis.

3.3 Inulin hydrolytic hydrogenation

The magnetically recoverable 5 % Ru-Fe$_3$O$_4$-SiO$_2$ catalyst was also tested in the hydrolytic hydrogenation of inulin to mannitol. The maximum mannitol selectivity reached in the work was 44.3 %, slightly higher than the result obtained with the 1 % Ru/C catalyst (40 %). Depending on the test conditions, the liquid phase of the catalysate can contain, in addition to mannitol, sorbitol (selectivity of up to 15 %), glycerol (up to 6.5 %), EG (up to 4 %), PG (up to 5 %), and other polyhydric alcohols in trace amounts. In our studies, we selected the optimum values of the main process parameters: temperature, reaction time, hydrogen partial pressure, and Ru:inulin ratio. Figure 3a shows the effect of the test temperature on the selectivity toward mannitol and the secondary reaction products in the range of 140–180 °C.

(a)   (b)
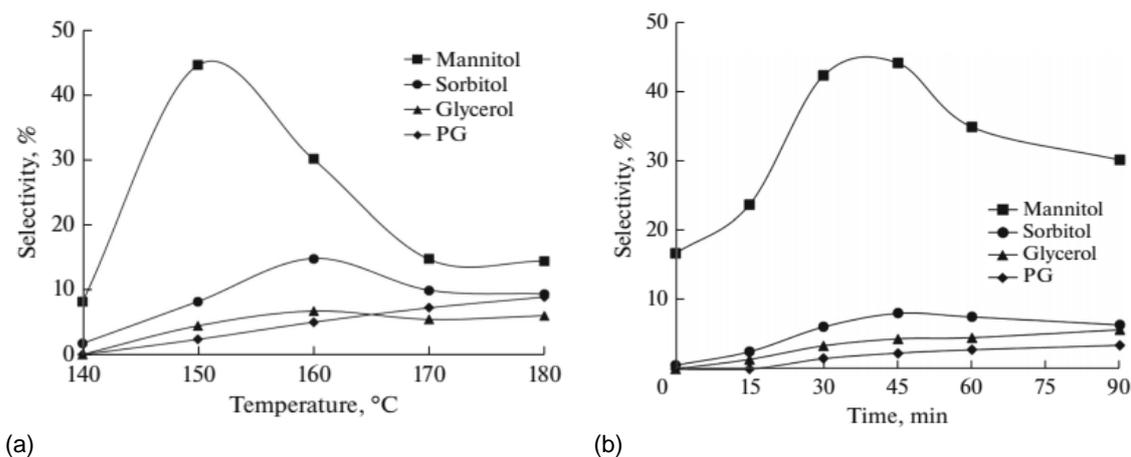
Figure 3: (a) Dependence of selectivity toward mannitol, sorbitol, glycerol, and PG on the process temperature (0.1167 mmol of Ru per gram of inulin; 0.3 g of inulin; 0.07 g of catalyst; 30 mL of H$_2$O; H$_2$ 60 bar; 45 min) (b) Dependence of selectivity toward mannitol and secondary products on process time (0.1167 mmol of Ru per gram of inulin; 0.3 g of inulin; 0.07 g of catalyst; 30 mL of H$_2$O; 150 °C; H$_2$ 60 bar)

Figure 3b shows our results from studying the dependence of the selectivity toward mannitol and other products on the process time. The highest mannitol selectivity was observed at a reaction time of 45 min. We determined the optimum values of H$_2$ partial pressure (60 bar) and the Ru:inulin ratio (0.1167 mmol of Ru in the catalyst's composition per gram of inulin). To study the catalyst's stability, it was separated from the reaction mass using a neodymium magnet and used in the next test. The results show that the selectivity of mannitol and the productivity of the catalyst remained virtually the same, testifying to the catalyst's stability in the hydrolytic hydrogenation of inulin.

4. Conclusions

It was shown that magnetically recoverable Rucontaining catalysts can be used in the one-pot conversion of such natural polysaccharides as cellulose and inulin to the high added-value products EG and PG (cellulose) and mannitol (inulin). The effect of the reaction parameters on the selectivity toward the main products was studied. In the hydrogenolysis of cellulose, the highest selectivities for EG (19.1 %) and PG (20.9 %) are achieved within 50 min under conditions of 255 °C, H$_2$ 60 bar, 0.1167 mmol of Ru in the catalyst composition per gram of cellulose, and 0.195 mol of Ca(OH)$_2$ per mole of cellulose. The conversion of cellulose is 100 %. In the hydrolytic hydrogenation of inulin, maximum mannitol selectivity (44.3 %) is reached within 45 min under conditions of 150 °C, H$_2$ 60 bar, and 0.1167 mmol of Ru in the catalyst composition per gram of inulin. The conversion of inulin is 100 %. The experiments were performed in triplicate. The value of the standard error of the experiment does not exceed 4.1 %. Our results, the stability of the 5 % Ru-Fe$_3$O$_4$-SiO$_2$ catalyst under hydrothermal conditions, and the easy way in which the catalyst can be separated from the reaction mixture using an external magnetic field make this catalyst promising for industrial application in the biomass conversion to high added-value chemicals and feedstock for biofuel production.

1158

References

Alva G., Lin Y., Fang G., 2018, An overview of thermal energy storage systems, Energy, 144, 341–378.

Bereczki D., Liu M., Fernandes do Prado G., Fekete I., 2007, Mannitol for acute stroke, Cochrane Database of Systematic Review, 3, CD001153.

Budavari S. (ed.)., 1996, The merck index - an encyclopedia of chemicals, drugs, and biologicals, whitehouse station, Merck and Co., Inc., NJ, USA.

Guivar J.A.R., Martinez A.I., Anaya A.O., De Los Santos Valladares L., Felix L.L., Dominguez A.B., 2014, Structural and magnetic properties of monophasic maghemite (γ-Fe_2O_3), nanocrystalline powder, AdvAnces in Nanoparticles, 3, 114–121.

Harlin A., 2011, Biogenic precursors for polyphenol, polyester and polyurethane resins. In Handbook of Bioplastics and Biocomposites Engineering Applications, Pilla, S., Ed. Scrivener Publishing: Salem, MA, USA.

Heinen A.W., Peters J.A., van Bekkum H., 2001, The combined hydrolysis and hydrogenation of inulin catalyzed by bifunctional Ru/C, Carbohydrate Research, 330, 381–390.

Imhof P.J., 2013, Van der Waal in: Catalytic process development for renewable materials, Wiley-Vch Weinheim, Germany.

Lawson P., 2007, Mannitol, Blackwell Publishing Ltd, 219–225.

Manaenkov O.V., Kislitsa O.V., Matveeva V.G., Sulman E.M., Sulman M.G., Bronstein L.M., 2019, Cellulose conversion into hexitols and glycols in water: recent advances in catalyst development, Frontlers in Chemistry,7, 834–841.

Manaenkov O., Mann J., Kislitza O., Losovyj Y., Stein B., Morgan D., Pink M., Lependina O., Shifrina Z., Matveeva V., Sulman E., Bronstein L., 2016, Ru-containing magnetically recoverable catalysts: a sustainable pathway from cellulose to ethylene and propylene glycols, ACS Applied Material Interfaces, 8, 21285-21293.

Matveeva V.G., Sulman E.M., Manaenkov O.V., Filatova A.E., Kislitza O.V., Sidorov A.I., Doluda V.Y., Sulman M.G., Rebrov E.V., 2017, Hydrolytic hydrogenation of cellulose in subcritical water with the use of the Ru-containing polymeric catalysts, Catalysis Today, 280, 45–50.

Mayuri Omae J., Goto P.A., Rodrigues L.M., Santos S.S., Moser Paraiso C., Madrona G., Bergamasco R.D.C., 2017, Beetroot extract encapsulated in inulin: storage stability and incorporation in sorbet, Chemical Engineering Transactions, 57, 1843–1848.

Ohrem H.L., Schornick E., Kalivoda A., Ognibene R., 2014, Why is mannitol becoming more and more popular as a pharmaceutical excipient in solid dosage forms? Pharmaceutical Development Technologies, 19(3), 257–262.

Okoromah C.A., Afolabi B.B., Wall E.C., 2011, Mannitol and other osmotic diuretics as adjuncts for treating cerebral malaria, Cochrane Database of Systematic Reviews, 4, CD004615.

Pinheiro Oliviera R.D.S., Perego P., Nogueira De Oliviera M., Converti A., 2011, Growth and survival of mixed probiotics in nonfat fermented milk: the effect of inulin, Chemical Engineering Transactions, 24, 457–462.

Prabhakar H., Singh G.P., Anand V., Kalaivani M., 2014, Mannitol versus hypertonic saline for brain relaxation in patients undergoing craniotomy, Cochrane Database of Systematic Reviews, 7:CD010026.

Rinaldi R., 2014, Catalytic hydrogenation for biomass valorization, RSC Publishing, Cambridge, GB.

Sugiyama S., Tanaka H., Bando T., Nakagawa K., Sotowa K.-I., Katou Y., Mori T., Yasukawa T., Ninomiya W., 2013, Liquid-Phase oxidation of propylene glycol using heavy-metal-free Pd/C under pressurized oxygen, Catalysis Today, 203, 116–121.

Wang D., Astruc D., 2014a, Fast-growing field of magnetically recyclable nanocatalysts, Chemical Reviews, 114(14), 6949–6985.

Wang D., Astruc D., 2014b, Magnetically recoverable ruthenium catalysts in organic synthesis. Molecules, 19, 4635–4653.

Yue H., Zhao Y., Ma X., Gong J., 2012, Ethylene glycol: properties, synthesis, and applications, Chemical Society Reviews, 41(11), 4218–4244.

Zhang J., Wu S., Liu Y., 2014, Direct conversion of cellulose into sorbitol over a magnetic catalyst in an extremely low concentration acid system, Energy & Fuels, 28, 4240–4246.